



## Electroconductive coatings on porous ceramic supports

B.J. BLADERGROEN, A. MALULEKE and V.M. LINKOV\*

*Inorganic Porous Media Group, Department of Chemistry, University of the Western Cape, P. Bag X17, Bellville, 7535, South Africa*

(\*author for correspondence, fax: + 27 21 9592218, e-mail: vlinkov@uwc.ac.za)

Received 14 October 2002; accepted in revised form 25 February 2003

**Key words:** electrically conductive coatings, electroless plated nickel, porous ceramic support, pyrolytic carbon, sputtered gold, water permeability

### Abstract

The preparation of porous conductive coatings on porous ceramic supports for potential use in electrosynthesis, anodic decomposition of organic compounds and electrosorption units is described. The prepared conductive coatings on porous ceramic supports consisted either of carbon, gold or nickel, or a combination of carbon and gold. Carbon coatings were obtained by pyrolytic decomposition of liquid petroleum gas (LPG), gold was sputter coated and nickel coatings were formed by electroless plating. The permeability for water and electrical resistance of each coated support were measured and compared. Pyrolytic carbon was deposited throughout the support whereas the nickel and gold coatings were formed on the outer surface of the support. The resistance of a carbon coating could be regulated between 0.5 and 2  $\Omega \text{ cm}^{-1}$  of support while the permeability of the carbonized support was as high as 75% of the permeability of the unmodified support. The nickel and gold coatings had no significant effect on the permeability and could be prepared with a resistance of 0.25 and 1  $\Omega \text{ cm}^{-1}$  of support, respectively.

### 1. Introduction

The preparation of porous electrodes is of interest for processes such as electrosynthesis, anodic decomposition of organic pollutants and electrosorption that requires a large electrochemically active area with intensive contact between reactants and electrode surface. For these applications the production of an electrode at minimal cost, with optimal hydrodynamic properties, mechanical and chemical stability and sufficient electrochemical activity is essential. Noble metals are known to be chemically stable and exhibit good electroconductive and electrocatalytic properties [1, 2] but are very expensive. Instead of manufacturing a porous electrode from these expensive materials, the production cost of a porous electrode may be minimized by coating a suitable, cheaper porous matrix with a coating of electroconductive material. In this work, a porous ceramic support is chosen as a suitable matrix because of its relatively low cost, high surface area and high chemical and mechanical stability.

The prepared porous electrodes were developed as part of a larger project on the development of an electrosorption membrane, which combines the properties of electrosorption electrodes and microfiltration membranes [3, 4]. An electrosorption process can be viewed as an ion exchange bed process in which the resin is electrically regenerated. Such systems consist of an electrochemical cell with two electrodes of which at least

one contains incorporated ion exchange resin and is permeable to water. When a d.c. voltage is applied between two electrodes, protons and hydroxyl ions are generated by electrolysis at the surface of the anode and cathode, respectively. Hydroxyl ions and protons are used to activate or regenerate the ion exchange sites on the electrode. The electrosorption electrode is prepared by impregnating a porous electrode with ion exchange material. This desired porous electrode has to meet the following requirements:

- (i) The conductive coating should have low electrical resistance to minimize the potential drop over the axial length of the electrode during the electrolytic process.
- (ii) The coated substrate must be permeable and the pores of the substrate must remain accessible for the sorption phase that will subsequently be incorporated. The incorporation of sorption material will be discussed in a future paper.
- (iii) The porous electrode must exhibit high catalytic activity towards water electrolysis.
- (iv) The conductive coating should have high chemical stability under anodic and cathodic conditions.

Thin noble metal coatings may suit the requirements mentioned above very well. Instead of preparing a continuous layer of the noble metal (to obtain electrical conductivity) a more economical approach would be to use a fraction of this expensive material in highly

dispersed form on top of a cheaper conductive coating to obtain high electrocatalytic activity.

Deposition of highly dispersed carbon in the form of an electroconductive coating has been described previously [5, 6] and showed promising stability and conductive properties. Carbon was therefore selected as one of the materials for electroconductive coatings. Besides carbon, nickel and gold were also tested as potential electrode materials. The preparation of both nickel [7–11] and copper [11] coatings on nonconductive substrates is well described. Nickel was chosen for its low overpotential for the oxygen evolution reaction [12] (lowest among the non-noble metal materials). Gold is an excellent electroconductive material and coatings of gold are extensively used as conductive layers [13]. Gold is relatively stable and cheaper than platinum or palladium. The potential usefulness of the various coating materials for electrosorption supports may be determined by a combination of factors such as electrical resistance, electrochemical stability and the effect on the permeability of the initial substrate.

## 2. Experimental details

The preparation of electroconductive coatings using carbon, gold or nickel will be discussed separately. Two different types of support were used as a matrix for the coatings. Details of the unmodified supports are given in Table 1. The permeability of the substrates was measured before and after coating, using the dead end method [14]. The electrical resistance was measured over a distance of 5 cm in the axial direction of the support using a Fluke 73 multimeter. Morphology was studied using scanning electron microscopy (SEM). Elemental analysis was done using energy dispersive X-ray spectroscopy (EDX). The electrochemical stability of the electroconductive coatings was tested with cyclic voltammetry, using an Auto PGST-30 potentiostat/galvanostat instrument (ECO Chemie BV, The Netherlands). By changing the electrode from anode to cathode for several hundreds of cycles in 0.5 M  $\text{Na}_2\text{SO}_4$ , the test method simulated the conditions of the sorption electrode in real life operation. A platinum wire and a saturated calomel electrode were used as counter and reference electrodes, respectively. The current density is given in  $\text{A cm}^{-2}$ .

Table 1. Main characteristics of the unmodified tubular porous aluminium oxide element

| Support type   | I       | II      |
|--|---------|---------|
| Outer diameter (mm)  | 10      | 10      |
| Inner diameter (mm)  | 7       | 7       |
| Average pore size ( $\mu\text{m}$ )  | 0.9     | 3       |
| Porosity (%)   | 40–45   | 40      |
| Permeability ( $\text{m}^3 \text{ m}^{-2} \text{ bar}^{-1} \text{ h}^{-1}$ ) | 2.5–2.6 | 4.2–4.3 |
| Length (mm)  | 105     | 105     |

## 2.1. Preparation methods

### 2.1.1. Carbon coating

Ceramic substrates were coated with carbon by pyrolytic decomposition of methane (analytical grade, Afrox) or liquid petroleum gas (LPG) gas (Afox). The coatings procedure was as follows. A support was placed in the middle of a quartz tube (dia. 5 cm) and centred with a mild steel wire to prevent the support from touching the tube. Subsequently, the quartz tube was put in a tube furnace. The pyrolytic gas was fed from one side into the tube at a flowrate of  $50 \text{ ml min}^{-1}$ . To optimize the coating conditions, carbonization was done at temperatures between 700 and 900 °C while the duration of the experiment varied from 30 to 300 min.

### 2.1.2. Nickel coating

Ceramic substrates were coated with nickel by electroless plating [7]. Prior to plating, the substrates were activated using a  $\text{Sn}^{2+}$  and a  $\text{Pd}^{2+}$  solution. Both solutions were prepared by adding 0.1 g  $\text{SnCl}_2 \cdot 2\text{H}_2\text{O}$  and  $\text{PdCl}_2$ , respectively, to 10 ml of 0.1 M HCl. Ultra-pure water was added to the 100 ml mark. The supports were initially submerged in the  $\text{SnCl}_2$  solution for 5 min and then rinsed with deionized water. Subsequently the supports were submerged in the  $\text{PdCl}_2$  solution for 5 min and rinsed with deionized water. These steps were

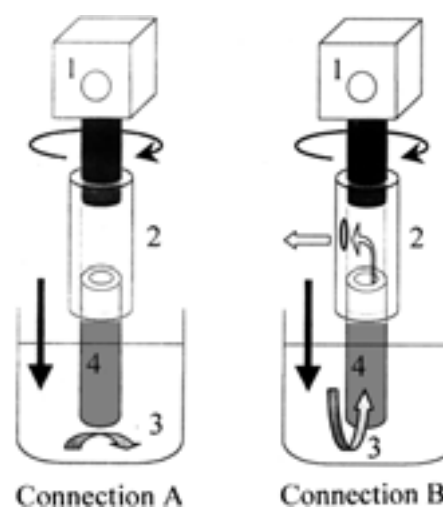


Fig. 1. Reaction set-up with connection A and B for electroless nickel plating: (1) overhead stirrer, (2) silicon tubing, (3) plating solution and (4) porous ceramic support.

Table 2. Composition of the nickel plating bath

| Compound   | Concentration         |
|--|-----------------------|
| $\text{NiSO}_4 \cdot 6\text{H}_2\text{O}$                      | $31 \text{ g l}^{-1}$ |
| $\text{NaPH}_2\text{O}_2$                                      | $54 \text{ g l}^{-1}$ |
| $(\text{CH}_3\text{COO})_2\text{Pb} \cdot 3\text{H}_2\text{O}$ | 5 ppm                 |
| Lactic acid  | $50 \text{ g l}^{-1}$ |
| Acetic acid  | $38 \text{ g l}^{-1}$ |
| pH   | 4.5                   |

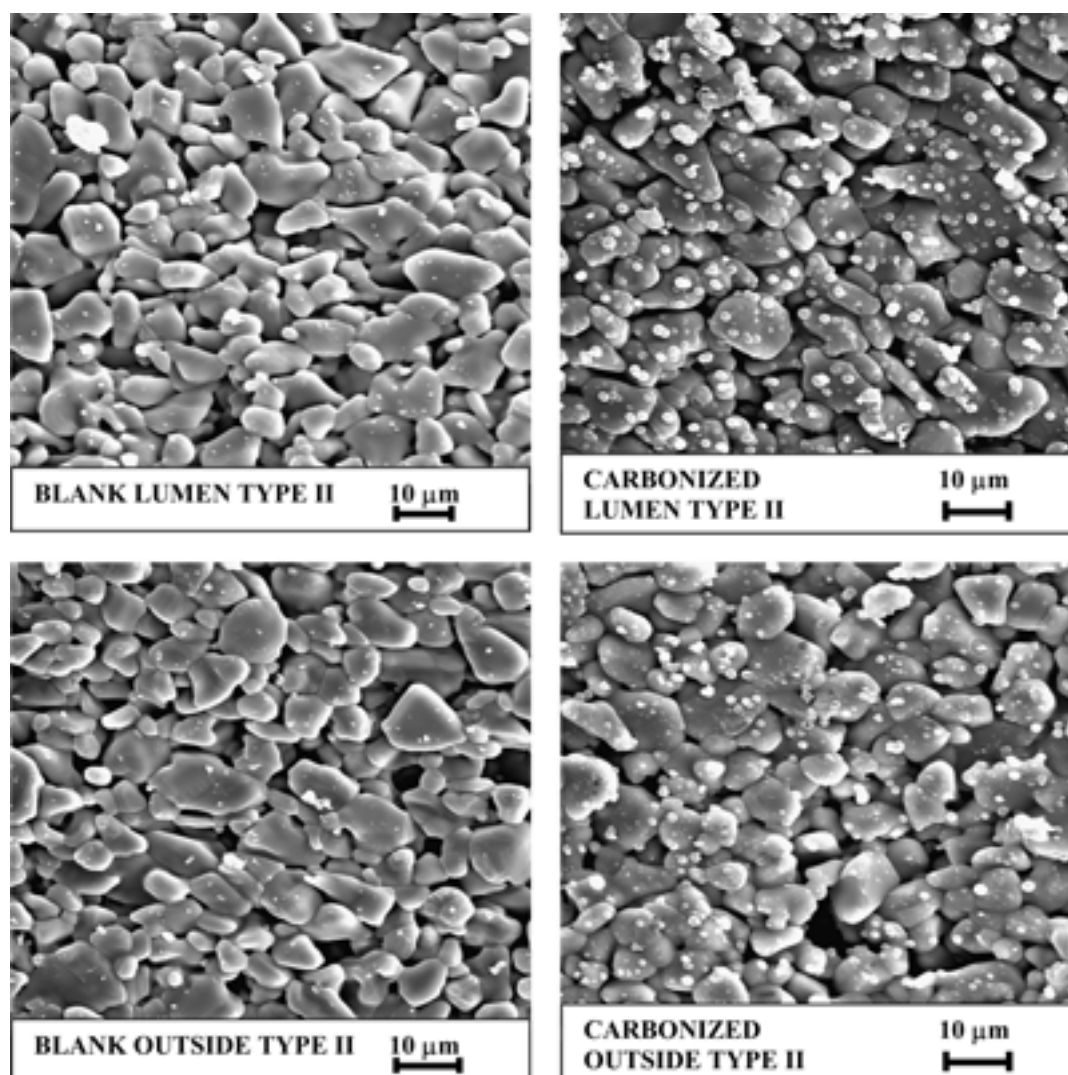


Fig. 2. SEM images of blank support (left side) and carbon coated supports (right side). (A) Outer side, (B) carbonized outer side, (C) lumen side and (D) carbonized lumen side.

Table 3.

| Support | Type | Treatment   | Pyrolytic gas | $T$<br>/°C | Time<br>/min | Permeability<br>/ $\text{m}^3 \text{m}^{-2} \text{bar}^{-1} \text{h}^{-1}$ | %   | Resistance<br>/ $\Omega \text{cm}^{-1}$ |
|---------|------|-------------|---------------|------------|--------------|--|-----|---|
| 1       | I    | none        | —             | —          | —            | 2.5  | 100 | >1000                                   |
| 2       | II   | none        | —             | —          | —            | 4.2  | 100 | >1000                                   |
| 3       | II   | carbonized  | methane       | 800        | 150          | 3.9  | 93  | >1000                                   |
| 4       | II   | carbonized  | methane       | 900        | 150          | 3.7  | 88  | >500                                    |
| 5       | II   | carbonized  | LPG           | 800        | 150          | 3.0  | 71  | 95                                      |
| 6       | II   | carbonized  | LPG           | 900        | 150          | 0.21   | 5   | 0.6                                     |
| 7       | II   | carbonized* | LPG           | 900        | 150          | 1.1  | 26  | 0.5                                     |
| 8       | II   | carbonized* | LPG           | 900        | 30           | 3.2  | 75  | 2.0                                     |
| 9       | I    | carbonized* | LPG           | 850        | 150          | 1.5  | 60  | 3                                       |
| 10      | I    | carbonized* | LPG           | 900        | 150          | 0.55   | 23  | 0.5                                     |
| 11      | I    | carbonized* | LPG           | 900        | 30           | 1.7  | 67  | 2.3                                     |

\* Supports rapidly removed from the hot furnace after pyrolysis.

repeated five times before the support was dried in a furnace at 120 °C for 12 h. After activation, the supports were connected to an overhead stirrer using connection A or B as illustrated in Figure 1. While rotating slowly, the support was submerged in 10 ml

nickel plating solution at various temperatures (between 60 and 95 °C) for various times (5 to 15 min). The composition of the plating bath is shown in Table 2.

When connection A was used, trapped air inside the support prevented the plating solution from entering the

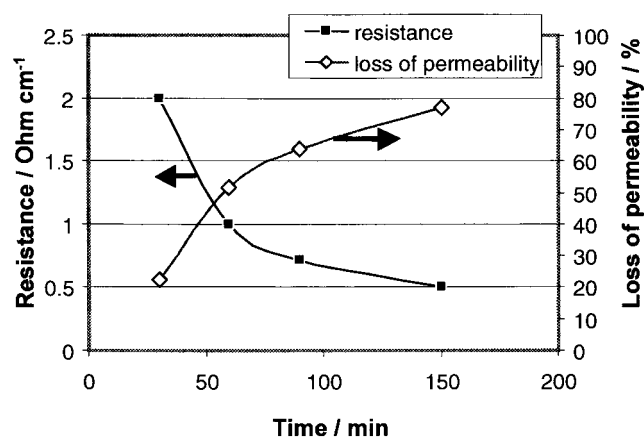


Fig. 3. Effect of pyrolysis time at 900 °C using LPG on permeability and resistance.

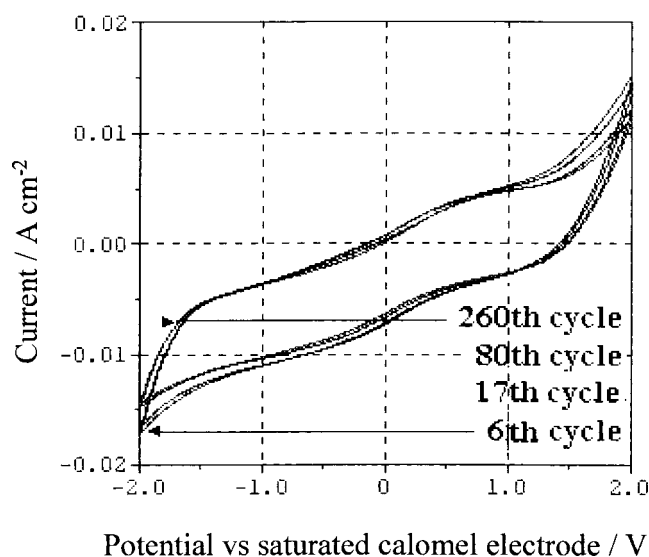


Fig. 4. Stability of carbon coating, cyclic voltammetry 0.05 V s<sup>-1</sup> in 0.5 M Na<sub>2</sub>SO<sub>4</sub>.

lumen side of the support. When connection B was used, the plating solution could enter the lumen side as the air inside the support could escape via the hole in the silicon tube that connected the support to the stirrer (Figure 1).

### 2.1.3. Gold coating

Ceramic substrates were coated with gold using an Edwards S 150B sputter coater. The argon pressure in the sputter chamber and the potential difference between the cathode and the anodic gold plate were set to

0.04 kPa argon and 1 kV. The deposition time was varied from 3 to 10 min. After this first period of gold deposition, the substrates were turned around and sputtered for the same period of time to ensure that even coating was obtained.

## 2.2. Results and discussion

The properties of the carbon, nickel and gold coated supports were determined by characterizing their permeability, resistance, uniformity of the deposited electroconductive phase and the electrochemical stability. The characteristics of the different coatings will be discussed separately.

### 2.2.1. Carbon coating

Over 95% of the carbon coated supports had a homogeneous dark gray appearance. No colour difference existed between lumen, outer surface or cross section of the tube. The SEM images of the supports before and after carbonization look very similar (compare Figure 2A/C with 2B/D, respectively). The only difference was small white particles (1 μm in size) on the lumen and outside of the carbonized membrane. These dots were most probably carbon particles. However, these particles do not play a significant role in the total electroconductivity of the membrane since their number is too small and the distance between the particles is too large. The actual conductive layer is too thin and smooth to be detected by SEM.

Some supports showed areas where no carbon was deposited even after a relatively long pyrolysis time (5 h). The shape and size of these uncarbonized areas were irregular. The cause of the formation of such uncoated areas was possibly due to minor intrinsic differences in composition of the untreated support as the irregularities were only seen on lengths of supports that had been cut from the same tube.

The effects of carbon deposition on the permeability and the conductivity of a ceramic support are shown in Table 3. Conditions for supports 3, 4 and 5 were replicated once whereas conditions for supports 6, 7, 8, 9 and 10 were replicated three or more times. The average values obtained from the replicated studies are given. The results show that the conductive coating with lowest resistance was formed when LPG was used as a pyrolysis gas at 900 °C (support 7 and 10). When methane was used as pyrolysis gas no significant carbon

Table 4. EDX result on electroless nickel plated ceramic supports

| Support | Type | Connection used | Ni content (wt%) at |             |       |
|---------|------|-----------------|---------------------|-------------|-------|
|         |      |                 | outside             | through cut | lumen |
| 12      | I    | A               | 60                  | 0           | 0     |
| 13      | II   | B               | 55                  | 0           | 15    |
| 14      | II   | B*              | 54                  | 0           | 40    |

\* During the electroless plating the support was lifted out of the plating solution every 2 min.

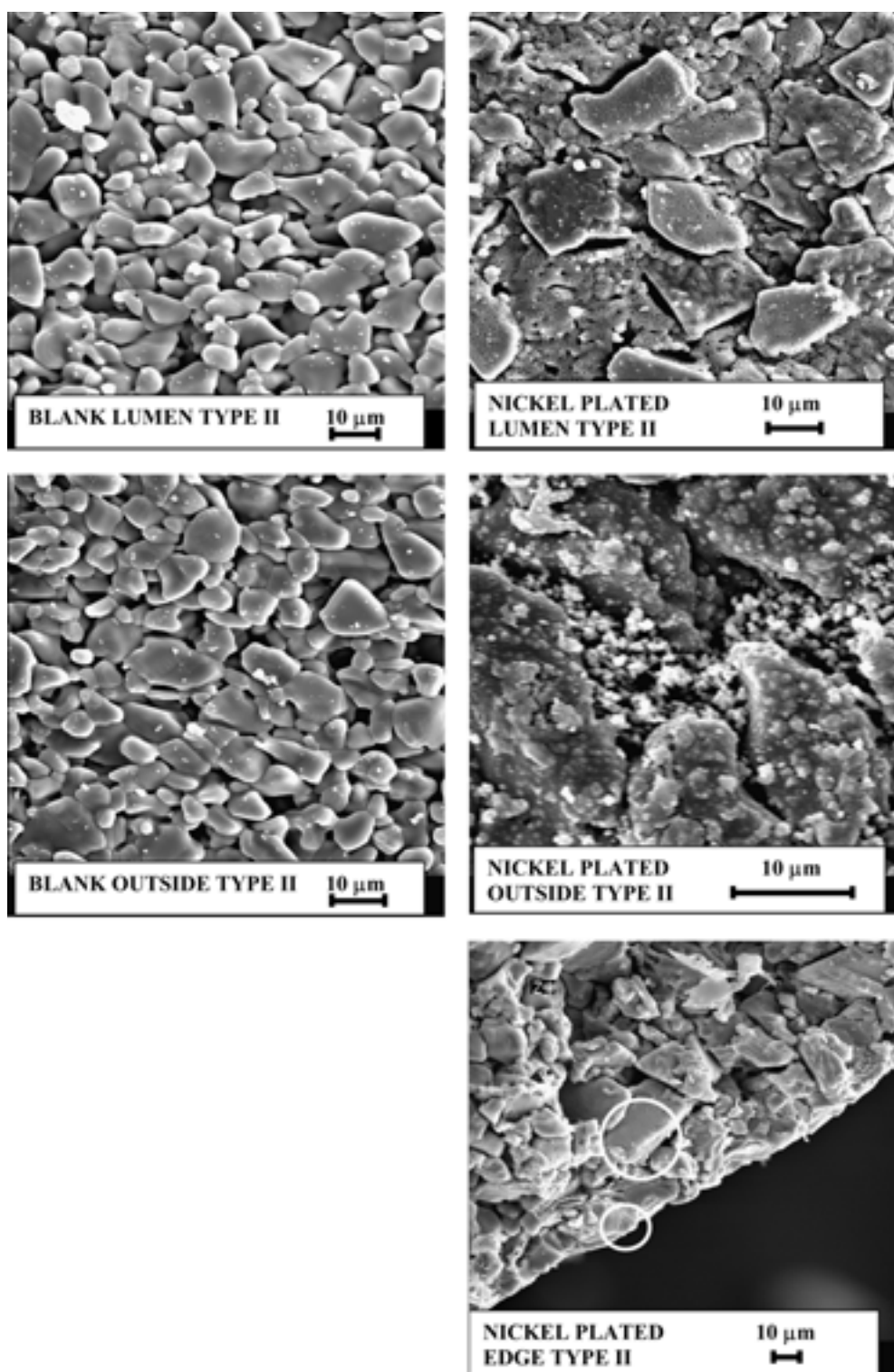


Fig. 5. SEM images of blank support (left side) and nickel coated supports (right side). (A) Outer side, (B) nickel plated outer side, (C) lumen side and (D) nickel plated lumen side.

deposition could be seen and the resistance of the support remained over  $500 \Omega \text{ cm}^{-1}$  at both pyrolysis temperatures (support 3 and 4). Higher temperatures than  $900^\circ\text{C}$  were not investigated as Belyakov et al. [5] indicated that structural changes of the ceramic surfaces (probably the formation of carbides or reduction of the oxides) were observed at higher temperatures. Table 3

also shows that the permeability can decrease drastically (95%) with decreasing resistance (see support number 6). However when the supports were removed from the furnace and cooled down outside the furnace after pyrolysis, significantly less permeability was lost (compare support 6 and 7). High molecular weight products that were formed during pyrolysis at temperatures below

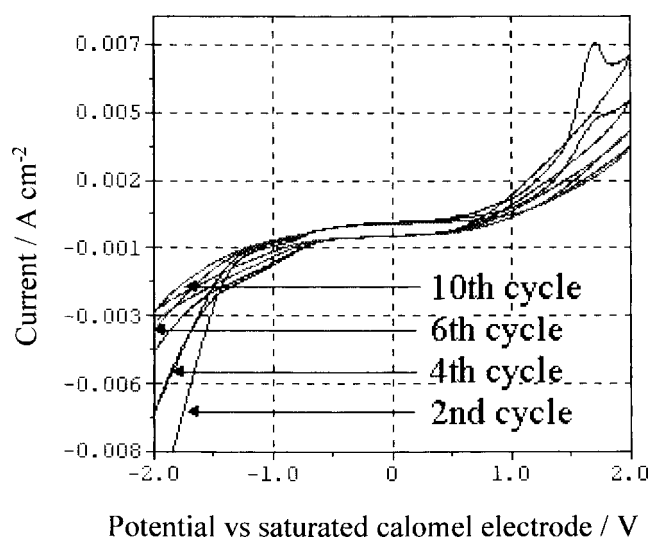


Fig. 6. Stability of nickel coating, cyclic voltammetry  $0.05 \text{ V s}^{-1}$  in  $0.5 \text{ M Na}_2\text{SO}_4$ .

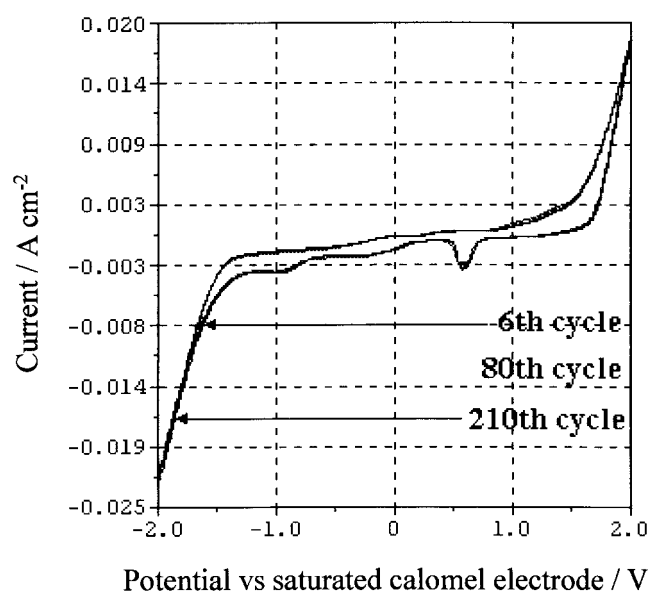


Fig. 7. Stability of gold coating, cyclic voltammetry  $0.05 \text{ V s}^{-1}$  in  $0.5 \text{ M Na}_2\text{SO}_4$ .

$700^\circ\text{C}$  and adsorbed onto the support during the cooling period may have been the cause for the significantly higher permeability drop. The influence of pyrolysis time on permeability drop and resistance is

shown in Figure 3. Resistance decreased at the expense of permeability. Cyclic voltammetry (CV) was used to show the stability of the carbon coating. Figure 4 shows scan 6, 20, 80 and 260 of the CV test. The height of the peaks at both sides of the figure (i.e., at a potential of  $-2$  and  $2 \text{ V}$  vs SCE) indicates the electrocatalytic activity of the electrode for water reduction and oxidation respectively. Within the first few scans the current density as a function of the potential decreased slightly (15% at  $-2 \text{ V}$  and 20% at  $2 \text{ V}$  vs SCE). No difference in current density as a function of the potential was observed between the 80th and the 260th scan, which means that the electrode becomes stable after some cycles.

### 2.2.2. Nickel coating

Porous nickel coatings with resistance of  $1 \Omega \text{ cm}^{-1}$  were prepared on the surface of ceramic supports. Bath temperatures below  $90^\circ\text{C}$  resulted in slow growth of the nickel layer. Acceptable nickel coatings were prepared at a bath temperature of  $92^\circ\text{C}$ .

For support 12 where connection A was used (Figure 1), a nickel layer was formed at the outside of the ceramic tubular support only. When connection B was used (support 13), a nickel coating was also formed at the lumen side of the support. To diminish the effect of depletion of nickel at the lumen side of the support, the support was lifted out of the solution (under  $\text{N}_2$  gas) every 2 min. This allowed the small volume of plating solution inside the support (with relatively low nickel content) to mix with the bulk of the plating solution containing a higher amount of nickel. Hence, more nickel could grow on the lumen side of support number 14, as is shown by the EDX results tabulated in Table 4. No nickel was found inside the pores of the support. The SEM results (Figure 5A/C before nickel coating and 5B/D after nickel coating) displayed a significant change in the appearance of the support surface. Some particles of the support were covered by larger nickel flakes. In these flakes fine pores were observed. Particles on the lumen side appeared significantly smaller than at the outer surface of the support. The edge of the support (see Figure 5E) showed only nickel deposited on the outer surface (see marked areas) of the support and no nickel inside the support.

Table 4 shows the resistance and permeability characteristics of nickel-coated supports. Electroconductive coatings were prepared with a resistance of about

Table 5. Permeability and conductivity characteristics before and after electroless nickel plating

| Support | Type | Treatment | Connection | Permeability<br>$/\text{m}^3 \text{ m}^{-2} \text{ bar}^{-1} \text{ h}^{-1}$ | Resistance $/\Omega \text{ cm}^{-1}$ |       |
|---------|------|-----------|------------|--|--------------------------------------|-------|
|         |      |           |            |  | outside                              | lumen |
| 1       | I    | none      |            | 2.7  | >1000                                | >1000 |
| 2       | II   | none      |            | 4.2  | >1000                                | >1000 |
| 12      | I    | Ni plated | A          | 2.7  | 1                                    | >1000 |
| 13      | II   | Ni plated | B          | 4.1  | 0.9                                  | 1000  |
| 14      | II   | Ni plated | B*         | 4.0  | 1.2                                  | 1.6   |

\* During the electroless plating the support was lifted out of the plating solution every 2 min.

Table 6. Permeability and conductivity characteristics before and after gold sputtering

| Support | Type | Treatment       | Permeability<br>/ $\text{m}^3 \text{m}^{-2} \text{bar}^{-1} \text{h}^{-1}$ | Resistance / $\Omega \text{cm}^{-1}$<br>outside support |
|---------|------|-----------------|--|---|
| 1       | I    | none            | 2.6  | >1000   |
| 2       | II   | none            | 4.2  | >1000   |
| 15      | I    | gold sputtering | 2.7  | 0.22  |
| 16      | II   | gold sputtering | 4.2  | 0.24  |

$1 \Omega \text{cm}^{-1}$  support with very low resistance to flow. The resistance of the coating at the lumen side could be reduced by lifting the support out of the solution every 2 min during the nickel plating experiment. Cyclic voltammetry scans were performed to obtain an impression of the stability of the nickel coating. Figure 6 shows scan 2, 4, 6 and 10. The rapid decrease of the current density of each subsequent cycle as function of the electrode potential indicated the instability of the nickel coating under the chosen conditions. The peaks occurring above 1 V vs SCE are related to the dissolution of nickel rather than the oxidation of water. This was confirmed by the development of the green colour of the solution during the experiment.

### 2.2.3. Gold coating

Gold coatings were formed on ceramic supports by ion beam sputtering. In general the gold coatings had a homogeneous appearance with slightly more gold deposited upon the side of the support that was facing the golden target. The resistance of the support coated for 3 min increased rapidly when currents over 100 mA were applied. The coatings prepared by sputtering for 10 min per side were stable when currents over 500 mA were applied.

Table 5 shows the resistance and permeability characteristics of gold-coated supports. Gold coatings were obtained with an electrical resistance as low as  $0.25 \Omega \text{cm}^{-1}$  with virtually no loss of permeability. In fact an increase in permeability was shown repeatedly. An increase of hydrophobicity of the support surface due to gold deposition could be the cause of the increased permeability.

The first 210 scans obtained with cyclic voltammetry for gold coated supports are shown in Figure 7. No decrease of current density as a function of the gold potential was observed during those cycles. The gold coating appeared to be very stable under the chosen conditions showing that the peaks at the potential of  $-2 \text{ V}$  and  $2 \text{ V}$  (vs SCE) are only related to the formation of  $\text{H}_2$  and  $\text{O}_2$ , respectively. The current densities at these potentials are higher than the current density obtained with carbon or nickel electrodes. The peak at  $0.5 \text{ V}$  vs SCE is probably related to  $\text{Au-O}$  reduction.

### 3. Conclusions

- (i) The resistance of a carbon coating could be regulated between  $0.5$  and  $2 \Omega \text{cm}^{-1}$  support maintaining a permeability as high as 75%. The position of the carbon coating was dispersed throughout the support with good electrochemical stability properties.
- (ii) The resistance of gold sputtered coatings was about  $0.25 \Omega \text{cm}^{-1}$  support. The permeability of the substrate increased between 0–5%. The stability of the gold coating was excellent when used as an anode or cathode in  $0.5 \text{ M Na}_2\text{SO}_4$  electrolyte solutions.
- (iii) The resistance of the electroless plated nickel coatings was about  $1 \Omega \text{cm}^{-1}$  support. The permeability of the substrate decreased between 0–5%. Depending on the experimental conditions the nickel coating could be formed on the outer and/or lumen side of the substrate. The nickel coating was unstable under testing conditions of cyclic voltammetry in  $0.5 \text{ M Na}_2\text{SO}_4$  electrolyte.

### References

1. C-H. Yang and T-C Wen, *Electrochim. Acta* **44** (1998) 207.
2. A.J. Dekker, 'Electroanalytical Chemistry: a Series of Advances' (New York Woods, R9(1), 1976).
3. B.J. Bladergroen and V.M. Linkov, *Sep. and Purif. Technol.* **25** (2001) 347.
4. B.J. Bladergroen and V.M. Linkov, 'Ceramic Membranes for Desalination and Filtration', *Filtration and Separation Magazine*, Sept. (2001).
5. V.M. Linkov and V. Belyakov, 'Support separation – Electroconductive Support', Progress Report Summary to Eskom (1997).
6. H. Moore, Tai-il Mah and P.W. Brown, *J. Am. Ceram. Soc.* **80**(5) (1997) 1285.
7. G.D. van den Berg, 'Electroless Plating of Selected Inorganic Substrates', MSc thesis, Potchefstroom University South Africa (1998).
8. Q. Li, S. Fan, W. Han, C. Sun and W. Liang, *J. Appl. Phys.* **36** (1997) 501.
9. K. Chen and Y. Chen, *Plat. Surf. Finish.* **84** (1997) 80.
10. M.V. Sullivan and H. Eigler, *J. Electrochem. Soc.* **104** (1957) 226.
11. D. Baudrand, *Plat. Surf. Finish.* **82** (1995) 57.
12. O.R. Stanford and K. Supra, *US Patent 4 567 274* (1985).
13. H. Honma, A. Hasegawa and S. Hotta, *Plat. Surf. Finish.* **82** (1995) 89.
14. M. Mulder, 'Basic Principles of Support Technology', (Kluwer Academic, London, 2nd edn, 1996), p. 474.